JACC Vol. 30, No. 6
November 15, 1997:1472–7

Reduced Myocardial Flow Reserve in Non–Insulin-Dependent Diabetes Mellitus

IKUO YOKOYAMA, MD, SHIN-ICHI MOMOMURA, MD, TOHRU OHTAKE, MD, KATSUNORI YONEKURA, MD, JUNICHI NISHIKAWA, MD, YASUHITO SASAKI, MD, MASAO OMATA, MD

Tokyo, Japan

Objectives. **We analyzed myocardial flow reserve (MFR) in patients with non–insulin-dependent (type II) diabetes mellitus (NIDDM) without symptoms and signs of ischemia.**

Background. **Diminished MFR in diabetes has been suggested. However, it remains controversial whether MFR is related to glycemic control, mode of therapy or gender in NIDDM.**

Methods. **Myocardial blood flow (MBF) was measured at baseline and during dipyridamole loading in 25 asymptomatic, normotensive, normocholesterolemic patients with NIDDM and 12 age-matched control subjects by means of positron emission tomography and nitrogen-13 ammonia, after which MFR was calculated.**

Results. **Baseline MBF in patients with NIDDM ([mean ± SD] 74.0 ± 24.0 ml/min per 100 g body weight) was comparable to that in control subjects (73.0 ± 17.0 ml/min per 100 g). However, MBF during dipyridamole loading was significantly lower in patients with NIDDM (184 ± 99.0 ml/min per 100 g, $p < 0.01$) than in control subjects (262 ± 120 ml/min per 100 g), as was MFR (NIDDM: 2.77 ± 0.85; control subjects: 3.8 ± 1.0, $p < 0.01$). A significantly decreased MFR was seen in men (2.35 ± 0.84) compared with women with NIDDM (3.18 ± 0.79, $p < 0.05$); however, no significant differences were found in terms of age, hemoglobin a1c and baseline MBF. MFR was comparable between the diet (2.78 ± 0.80) and medication therapy groups (2.76 ± 0.77) and was inversely correlated with average hemoglobin A1c for 5 years ($r = -0.55$, $p < 0.01$) and fasting plasma glucose concentration ($r = -0.57$, $p < 0.01$) but not age or lipid fractions.**

Conclusions. **Glycemic control and gender, rather than mode of therapy, is related to MFR in NIDDM.**

(J Am Coll Cardiol 1997;30:1472–7)

It has been widely recognized that maximal myocardial vasodilatory capacity can decrease in accordance with the severity of coronary stenosis (1). However, recent investigations have implicated several other factors in such alterations (2–9). Maximal myocardial vasodilatory capacity has been reported to be reduced in angiographically normal coronary arteries, especially in patients with diabetes mellitus (4,5). However, most of the diabetic patients in these studies also had systemic hypertension, and the role of hypertension in reduced flow reserve in these patients is not yet known. Therefore, it is uncertain whether diabetes alone decreases maximal myocardial vasodilatory capacity or if hypertension also has such an effect (10). Glycemic control is important in the management of diabetes mellitus because of its possible relation to vascular complications. For example, a linear relation between glycemic control and microangiopathy, neuropathy or retinopathy in patients with insulin-dependent (type I) diabetes mellitus has been reported (11). Furthermore, a linear relation between the incidence of death from coronary artery disease and glycemic control in patients with non–insulin-dependent (type II) diabetes mellitus (NIDDM) has been shown (12). However, the relation between glycemic control and blood flow abnormality or maximal myocardial vasodilatory capacity in diabetic patients has not yet been clarified.

Positron emission tomography (PET) has emerged as a new technology to measure tissue metabolism as well as blood flow in vivo. Because this technology can estimate maximal myocardial vasodilatory capacity by evaluating myocardial flow reserve (MFR), noninvasive investigation of blood flow abnormality is now possible in patients with NIDDM.

Our study was undertaken first to determine whether MFR is decreased in patients with NIDDM without evidence of heart disease, hypertension or hypercholesterolemia through evaluation with PET using nitrogen-13 (N-13) ammonia and dipyridamole stress testing. If such a reduction was found, we planned to further investigate whether it was related to glycemic control, as determined by fasting blood sugar (glucose) concentration (FBS) and hemoglobin A1c (HbA1c), mode of therapy and gender in NIDDM.

From the Second Department of Internal Medicine and Department of Radiology, University of Tokyo, Tokyo, Japan. This work was supported by a Research Grant for Cardiovascular Disease (8A-5) from the Ministry of Health and Welfare, Tokyo, Japan.

Manuscript received November 27, 1996; revised manuscript received July 9, 1997, accepted August 5, 1997.

Address for correspondence: Dr. Ikuo Yokoyama, 7-3-1 Hongoh Bunkyo-ku, Second Department of Internal Medicine, University of Tokyo, Tokyo 113, Japan. E-mail: yokochan-cky@umin-tokyo.ac.jp.

0735-1097/97/$17.00
PII S0735-1097(97)00327-6

Abbreviations and Acronyms

ECG = electrocardiogram, electrocardiographic
FBS = plasma fasting blood sugar concentration
HbA1c = hemoglobin A1c
MBF = myocardial blood flow
MFR = myocardial flow reserve
NIDDM = non–insulin-dependent diabetes mellitus
PET = positron emission tomography (tomographic)

Methods

Study group. Twenty-five patients with NIDDM without hypertension, hypercholesterolemia or a history of ischemic heart disease (15 men, 10 women) were studied. Twelve normolipidemic, normoglycemic asymptomatic subjects (9 men and 3 women) without a history of heart disease served as control subjects.

The following criteria were used to diagnose NIDDM: FBS concentration >7.3 mmol/liter (140 mg/dl) and hemoglobin A1c >6.5% before the initiation of therapy. Fourteen patients were being treated with diet therapy alone (diet therapy group) and 11 were receiving oral hypoglycemic agents (sulfonylurea; medication therapy group), and the influence of the type of therapy on MFR was assessed. Patients treated with insulin were excluded because the mechanism of the disease process in insulin-dependent diabetes mellitus differs from that in NIDDM. Caffeine intake and theophylline-containing foods or drugs were prohibited for 24 h before the PET studies.

Table 1 summarizes the general characteristics of our study group. There were no significant differences in terms of age, gender, body weight, height, body mass index or blood pressure at rest and during dipyridamole administration; heart rate at rest and during dipyridamole loading; plasma concentration of total cholesterol; low density lipoprotein cholesterol; high density lipoprotein cholesterol; and plasma triglyceride concentration between the two groups. Plasma concentrations of FBS and hemoglobin A1c were significantly higher in those with NIDDM than in control subjects.

Results on the rest electrocardiogram (ECG) were normal in all study subjects. We performed a symptom-limited treadmill test for all subjects. Patients with typical chest pain or abnormal ECGs indicating myocardial ischemia were excluded. All study subjects were informed of the nature of the study, after which they agreed to participate in the protocol, which had been approved by the local Ethics Committee.

PET. Regional baseline myocardial blood flow (MBF) and that during dipyridamole administration was measured using PET and N-13 ammonia. Myocardial flow images were obtained using a Headtome IV scanner (Shimadzu Corp., Kyoto, Japan). This PET scanner has seven imaging planes; in-plane resolution is 4.5 mm at full width at half maximum, and the z-axial resolution is 9.5 mm at full width at half maximum. Effective in-plane resolution is 7 mm after using a smoothing filter. The sensitivities of the Headtome IV scanners are 14 and 24 kilocounts/s (μCi/ml) for direct and cross planes, respectively.

Table 1. Clinical Characteristics of Study Patients

	NIDDM Group (n = 25)	Control Group (n = 12)
Male/female	15/10	9/3
Age (yr)	58.9 ± 10.4	57.7 ± 12.2
Body weight (kg)	57.7 ± 10.4	61.7 ± 5.9
Height (cm)	161.3 ± 10.9	160 ± 7.00
BMI	22.2 ± 2.29	23.7 ± 2.5
HbA1c (%)	8.46 ± 1.88*	5.7 ± 0.26
FBS (mmol/liter)	9.0 ± 3.0*	4.9 ± 0.48
TC (mmol/liter)	5.02 ± 0.58	4.96 ± 0.61
HDL (mmol/liter)	1.38 ± 0.40	1.19 ± 0.82
TG (mmol/liter)	1.38 ± 0.89	1.35 ± 0.55
LDL (mmol/liter)	2.84 ± 0.90	2.89 ± 0.36
Rest		
SBP (mm Hg)	126 ± 14.1	125 ± 10.1
DBP (mm Hg)	75.8 ± 8.32	73.2 ± 6.9
HR (beats/min)	71.8 ± 10.4	73.6 ± 6.7
RPP (beats/min × mm Hg)	9,540 ± 1,633	9,173 ± 1,504
Dipyridamole		
SBP (mm Hg)	120 ± 16.1	116 ± 6.8
DBP (mm Hg)	69.9 ± 13.4	74.3 ± 6.9
HR (beats/min)	79.5 ± 12.2	83.6 ± 13.0
RPP (beats/min × mm Hg)	9,679 ± 1,540	9,603 ± 15

*$p < 0.01$ versus control group. Data presented are mean value ± SD or number of patients. BMI = body mass index; DBP = diastolic blood pressure; FBS = fasting plasma blood sugar concentration; HbA1c = hemoglobin A1c; HDL = high density lipoprotein cholesterol; HR = heart rate; LDL = low density lipoprotein cholesterol; NIDDM = non–insulin-dependent diabetes mellitus; RPP = rate–pressure product; SBP = systolic blood pressure; TC = total cholesterol; TG = triglycerides.

After acquiring transmission data to correct for photon attenuation before obtaining images, 15 to 20 mCi of N-13 ammonia was injected, and dynamic scanning with PET was performed for 2 min and static scanning with PET for 8 min. After waiting 45 min to allow for decay of the radioactivity of N-13 ammonia, dipyridamole (0.56 mg/kg body weight) was administered intravenously over 4 min. Five minutes after the end of administration of dipyridamole, 15 to 20 mCi of N-13 ammonia was injected, and, at exactly the same time, a second dynamic scan with PET was performed for 2 min and static scan for 8 min. The dynamic scan was performed every 15 s (eight times) in the 2-min period and dynamic data were obtained for seven slices. Only one-channel ECG monitoring in limb leads was made during the study with PET. Because standard electrodes for precordial ECG leads can absorb gamma X-rays, 12 lead ECGs were not obtained.

Determination of MBF and MFR. Regional MBF was calculated basically according to the two-compartment N-13 ammonia tracer kinetic model (13,14). Briefly, the two-compartment model contains a freely diffusible N-13 ammonia compartment in the vascular and extravascular spaces and a second compartment that contains the metabolically trapped N-13 label. As shown by Krivokapitch et al. (13), the two-compartment model uses the following formula:

$$\frac{dQF(t)}{dt} = -\frac{(K_1 + MBF) \times QF(t)}{0.8} + k_2 \times QT(t) + MBF \times Ca(t)\,, \quad [1]$$

$$\frac{dQT(t)}{dt} = \frac{K_1 \times QF(t)}{0.8} - k_2 \times QT(t)\,, \quad [2]$$

where K_1 (in ml/min per g) and k_2 (in min^{-1}) represent the forward and reverse rates for exchange between the two compartments; QF(t) is radioactivity in the freely diffusible space; QT(t) is radioactivity trapped in the myocardium; and Ca(t) is blood pool radioactivity. Because N-13 metabolites are assumed not to significantly convert back into freely diffusible space of the N-13 ammonia during the first 90 s of data acquisition, k_2 is nearly equal to zero. In contrast, the measured concentration by the tomograph Cm(t) is

$$Cm(t) = QF(t) + QT(t). \quad [3]$$

According to the experimental data, the relation between K_1 and MBF is as follows (13):

$$K_1 = (MBF/0.607)\, e^{(1.25/MBF)} - MBF. \quad [4]$$

The time activity curve of the left ventricular cavity was used as an input function. Tracer spillover was corrected by least-squares nonlinear regression analysis in our program to calculate the MBF with the assumption that myocardial and left ventricular radioactivity were influenced by each other. Specifically, true radioactivity of the left ventricular cavity at the time of $t(Ca(t)_{true})$ was expressed as follows:

$$Ca(t)_{true} = Ca(t)_{PET} - C_1{*}Cm(t)_{true}\,, \quad [5]$$

where $Ca(t)_{PET}$ is radioactivity of the left ventricular cavity measured by PET; $Cm(t)_{true}$ is the true radioactivity of the cardiac muscle; and C_1 is the spillover factor, which is expressed as a percentage with the assumption that C_1 (%) of the true radioactivity of the cardiac muscle was added to the radioactivity of the left ventricular cavity measured by PET. Similarly, true radioactivity of cardiac muscle at the time of $t(Cm(t)_{true})$ is expressed as follows:

$$Cm(t)_{true} = Cm(t)_{PET} - C_2{*}Ca(t)_{true}\,, \quad [6]$$

where $Cm(t)_{PET}$ is myocardial radioactivity measured by PET; $Ca(t)_{true}$ is the true radioactivity of the left ventricular cavity; and C_2 is the spillover factor, which is expressed as a percentage with the assumption that C_2 (%) of the true radioactivity of the left ventricular cavity was added to the myocardial radioactivity measured by PET. We determined C_1, C_2, MBF and the K_1 value by using equations 1 to 6 and least squares nonlinear regression analysis.

All data were corrected for dead time effects to reduce error to <1%. To avoid the influence of the partial volume effect associated with the objects' size, the relation between recovery coefficients and wall thickness obtained from experimental phantom studies in our laboratory was determined. For the correction of partial volume effect, wall thickness was measured with two-dimensional echocardiography by specialists in our hospital. The recovery coefficients estimated by myocardial wall thickness were taken into consideration in our program to measure MBF. For example, the recovery coefficient was 0.8 when myocardial wall thickness was 10 mm.

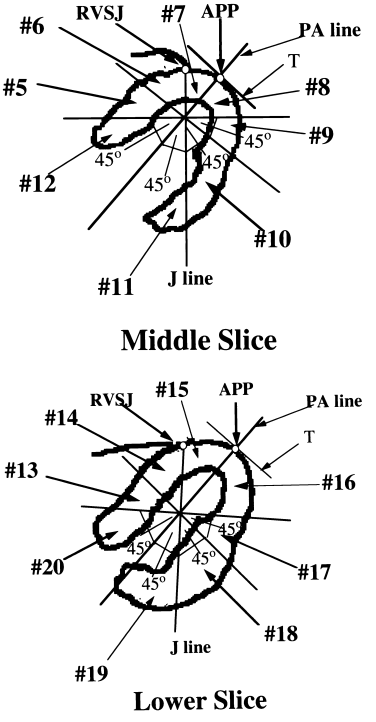

Figure 1. Schematic representation of placement of regions of interest and anatomic orientation of each segment on the transaxial images. Regions of interest were placed on the transaxial images as follows: For each slice, the anteroapical pole (APP) was determined visually, and a tangent to the anteroapical pole was drawn. Then a perpendicular line to the tangent from the anteroapical pole (PA line) was drawn from the anteroapical pole. The J line was drawn from the junction of the right ventricular wall and the septum (RVSJ) to the PA line at an angle of 45°. Based on the PA line and J line, the left ventricle was divided into eight segments equally. Septal segments were obtained from the middle transaxial slice (#5, #6) and lower slice (#13, #14), and anterior segments were obtained from the middle slice (#7, #8) and lower slice (#15, #16). Anteroseptal segments were defined as the left anterior descending coronary artery region. The lateral wall segment was obtained from the middle slice (#9, #10) and lower slice (#17, #18). Lateral segments were defined as the left circumflex coronary artery region. The inferoposterior wall segment was obtained from the middle slice (#11, #12) and lower slice (#19, #20). When #11, #12 of the middle slice was not large enough to place a region of interest, those segments were excluded in the data analysis. Inferoposterior segments were defined as the right coronary artery region.

MFR was determined by the ratio of MBF during dipyridamole loading to baseline MBF. Regions of interest were placed at the septum, anterior wall, lateral wall and inferoposterior wall on the transaxial images. Details are shown in Figure 1. To obtain input function, regions of interest were placed on the left ventricular cavity of each slice. To compare MFR, the average regional MBF was used.

Statistics. Baseline MBF, MBF during dipyridamole administration, MFR, body weight, systolic blood pressure, diastolic blood pressure, height, body mass index and lipid

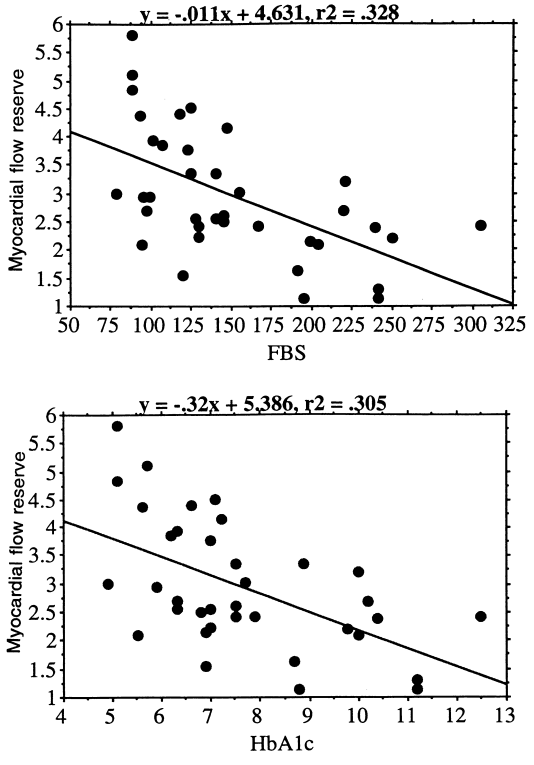

Figure 2. Top, Relation between MFR and FBS concentration for the previous 5 years in the entire study groups. **Bottom,** Relation between MFR and average HbA1c (%) for the previous 5 years in the entire study groups.

variables in the two groups were compared using analysis of variance, and then individual data were analyzed by the two-tailed Student *t* test. Values are expressed as the mean value ± SD. A value of $p < 0.05$ was considered significant.

Results

Hemodynamic and ECG responses to dipyridamole infusion. There were no significant differences in systolic blood pressure at rest and during dipyridamole administration and rate–pressure product between patients and control subjects (Table 1). During dipyridamole administration, typical chest pain or chest oppression accompanied by ECG changes was not observed in any study subject. Atypical chest pain, chest discomfort or dyspnea suggesting side effects of dipyridamole was observed in four patients without abnormal ECG changes.

Recording 12-lead ECG during PET is problematic because the absorbance of gamma X-rays by the standard electrodes could possibly influence PET measurements; therefore, a detailed description of ECG response to dipyridamole was not possible.

Baseline MBF and MBF during dipyridamole administration. In patients with NIDDM, baseline MBF (74.0 ± 24.0 ml/min per 100 g) was similar to that of control subjects (73.0 ± 17.0 ml/min per 100 g); however, it was significantly lower during dipyridamole administration (184 ± 99.0 vs. 262 ± 120 ml/min per 100 g, $p < 0.01$). MFR was significantly lower in patients with NIDDM (2.77 ± 0.85) than in control subjects (3.80 ± 1.00, $p < 0.01$). A significant decrease in MFR was seen in male (2.35 ± 0.84) compared with female patients with NIDDM (3.18 ± 0.79, $p < 0.05$), whereas age (57.5 ± 10.6 in men vs. 61.1 ± 10.2 in women), HbA1c (8.4 ± 1.8 in men vs. 8.7 ± 2.1 in women) and baseline MBF (70.0 ± 24.0 ml/min per 100 g in men vs. 80.0 ± 20.0 ml/min per 100 g in women) were comparable between the male and female patients with NIDDM. There was no significant regional difference in MFR in the patients or the control subjects (Table 2).

Mode of therapy and MFR. MFR in the diet therapy group (2.78 ± 0.80) was comparable to that in the medication therapy group (2.76 ± 0.77), and MFR in both groups was significantly lower in patients with NIDDM than in control subjects ($p < 0.01$). There were no significant differences in HbA1c and age between the diet therapy group and the medication therapy group (HbA1c: 8.2 ± 1.7 vs. 8.5 ± 2.0; age: 55.8 ± 10.7 vs. 61.6 ± 10.4, respectively), nor were there in systolic blood pressure (124 ± 8.86 vs. 129 ± 18.1 mm Hg), diastolic blood pressure (73.6 ± 9.75 vs. 76.4 ± 8.29 mm Hg) and rate–pressure product (8,586 ± 1,548 vs. 9,245 ± 1,470).

Relation between MFR and HbA1c, FBS and plasma lipid fractions. MFR correlated with FBS for the previous 5 years ($r = -0.57$, $p < 0.01$). There was a significant inverse correlation between MFR and average HbA1c for the previous 5 years in the entire study group (control subjects and patients with NIDDM) ($r = -0.55$, $p < 0.01$) (Fig. 2). However, there was no significant correlation between MFR and plasma lipid fractions or age and blood pressure in the entire study group.

Discussion

MFR in patients with NIDDM. Reduced maximal myocardial vasodilatory capacity in diabetes as assessed by coronary flow velocity has been reported (4,5). The existence of a microcirculation abnormality was suggested in human diabetic patients (4,5), as has been reported in animal experimental studies (15–18). However, because most of the patients used in those previous two studies had systemic hypertension, which can decrease MFR, it remained unclear whether MFR is typically decreased in patients with normotensive NIDDM without evidence of myocardial ischemia. Also, in those previous studies, flow reserve was measured with a Doppler catheter, which requires arterial cannulation (4,5), thus limiting the

Table 2. Comparison of Regional Myocardial Flow Reserve

	Myocardial Flow Reserve			
	Septum	Ant Wall	Lat Wall	Post Wall
Control group	3.95 ± 1.35*	3.84 ± 1.53*	3.61 ± 1.21*	3.80 ± 1.33*
NIDDM group	2.92 ± 0.89	2.82 ± 0.92	2.57 ± 0.90	2.77 ± 0.87

*$p < 0.01$ versus NIDDM group. Data presented are mean value ± SD. Ant = anterior; Lat = lateral; NIDDM = non–insulin-dependent diabetes mellitus; Post = posterior.

selection of study subjects. Moreover, a Doppler catheter can only measure coronary flow velocity and cannot achieve accurate measurement of MBF volume. Our selection of subjects, as well as the method of measurement used, differentiates our study from those previous studies.

Glycemic control is thought to be essential for the management of diabetes. For instance, recent studies have reported a hyperglycemia-induced angiopathy (19,20) and a linear relation between glycemic control and the incidence of death from coronary artery disease (12). The relation between retinopathy, neuropathy or nephropathy in diabetes and glycemic control has also been reported in insulin-dependent diabetes (11). However, it has not been clarified whether MFR is related to glycemic control in patients with NIDDM. We found reduced MFR without an increase in baseline MBF in such patients, and this abnormality was related to glycemic control and gender rather than mode of therapy. Furthermore, we found a significant inverse relation between MFR and the degree of long-term glycemic control in asymptomatic patients with NIDDM.

Because increased coronary resistance (21) and an attenuated response to reactive hyperemia with oral hypoglycemic agents (22,23) have been reported, those circumstances may influence maximal myocardial vasodilation in patients using oral hypoglycemic agents. However, no significant difference in flow reserve between patients on diet therapy and patients on medication therapy was reported in seven normotensive diabetic patients (5). In our present study, the significant inverse relation between MFR and long-term glycemic control suggests that MBF abnormalities in NIDDM are related to the degree of glycemic control rather than the mode of therapy. Our results and those of other investigators indicate that long-term glycemic control is essential for the management of vascular complications in patients with NIDDM. Extending these findings, the current report is the first of a relation between glycemic control and MFR.

MFR and lipid profiles, gender and age. Reduced MFR in patients with hyperlipidemia has been reported (8–10), as well as significantly greater reductions in MFR in male than in female patients with familial hypercholesterolemia (8). Therefore, the additional influence of hyperlipidemia on MFR in diabetes should be considered. However, in this study our patients were normocholesterolemic, so a significant relation between MFR and lipid levels would not be expected. We did, however, find that MFR in NIDDM was significantly lower in male than in female patients, and we believe that this is the first demonstration of a gender-specific variance in MFR in diabetes. Because our female study subjects were postmenopausal (mean age 61 years), the direct effect of estrogen on MFR can be considered negligible; however, the protective effect of estrogen during the premenopausal years may be related to this result. Although Czernin et al. (24) reported the influence of age on MFR, our patients were within a narrow age range; therefore, no correlation between age and MFR was expected in view of the design of the study.

Possible mechanism for the reduced MFR in NIDDM. With reference to the reports that showed diminished myocardial vasodilatory capacity in human diabetes (4,5), our results may in part be attributed to coronary microangiopathy, diffuse macrovascular atherosclerosis, as has been suggested by Mintz et al. (25), or abnormal endothelial function, or a combination of these. It is acknowledged that blood flow response to dipyridamole is considered endothelial independent. However, animal experimental studies suggest that endothelial dysfunction might also affect blood flow response to papaverine or dipyridamole (through flow-mediated vasodilation) (26–28). Therefore, an impairment of flow-mediated vasodilation (endothelial function) might account for this finding. In addition, balanced multivessel macrovascular disease without flow-limiting stenosis or differences in wall stress between patients and control subjects might also account for this finding.

Determination of MBF with N-13 ammonia PET. To determine MBF, we based our study on the two-compartment model using PET and N-13 ammonia, because this model has been well validated (13,14) and is frequently used in the assessment of MBF (8,9,24,29–35). Another model reported to measure MBF using PET and N-13 ammonia was a three-compartment model that considered metabolites of N-13 ammonia (36). However, animal experimental studies have shown that metabolites of N-13 ammonia can be negated during the first 90 s after N-13 ammonia injection (37,38). Therefore, accuracy of the measurement of MBF with N-13 ammonia PET and the two-compartment model is assured.

Conclusions. MFR was reduced in patients with NIDDM without evidence of ischemia. The inverse relation between MFR and HbA1c or FBS suggests that the degree of chronic glycemic control might be related to blood flow abnormality in patients with NIDDM, rather than the mode of therapy.

References

1. Gould KL, Lipscomb K. Effects of coronary stenoses on coronary flow reserve and resistance. Am J Cardiol 1974;34:48–55.
2. Camici PG, Chiriatti G, Lorenzoni R, Bellina RC, Gistri R, Italiani G. Coronary vasodilation is impaired in both hypertrophied and non-hypertrophied myocardium of patients with hypertrophic cardiomyopathy: a study with nitrogen-13 ammonia and positron emission tomography. J Am Coll Cardiol 1991;17:879–86.
3. Inoue T, Sasaki Y, Morooka S, et al. Coronary flow reserve in patients with dilated cardiomyopathy. Am Heart J 1993;125:93–8.
4. Nitenberg A, Valensi P, Sachs R, Dalim M, Aptecar E, Attali JR. Impairment of coronary vascular reserve and Ach-induced coronary vasodilation in diabetic patients with angiographically normal coronary arteries and normal ventricular systolic function. Diabetes 1993;32:1017–23.
5. Nahser PJ Jr, Brown RE, Oskarsson H, Winnifold MD, Rossen JD. Maximal coronary flow reserve and metabolic coronary vasodilation in patients with diabetes mellitus. Circulation 1995;91:635–40.
6. Uren NG, Crake T, Leffery DC, Silva R, Gavies GJ, Maseri A. Reduced coronary vasodilator function in infarcted and normal myocardium after myocardial infarction. N Engl J Med 1994;331:222–7.
7. Dayanikli F, Grambow D, Muzil O, Mosca L, Rubenfire M, Schwaiger M. Early detection of abnormal coronary flow reserve in asymptomatic men at high risk for coronary artery disease using positron emission tomography. Circulation 1994;90:808–17.
8. Yokoyama I, Murakami T, Ohtake T, et al. Reduced coronary flow reserve in familial hypercholesterolemia. J Nucl Med 1996;37:1937–42.

9. Yokoyama I, Ohtake T, Momomura S, Nishikawa J, Sasaki Y, Omata M. Reduced coronary flow reserve in hypercholesterolemic patients without overt coronary stenosis. Circulation 1996;94:3232–8.
10. Motz W, Straner BE. Improvement of coronary flow reserve after long term therapy with enalapril. Hypertension 1996;27:1031–8.
11. The Diabetes Control and Complications Trial Research Group. The effect of intensive treatment of diabetes on the development and progression of long term complications in insulin-dependent diabetes mellitus. N Engl J Med 1993;329:977–86.
12. Laakso M. Glycemic control and the risk for coronary heart disease in patients with non–insulin-dependent diabetes mellitus. Ann Intern Med 1996;124(1 Pt. 2):127–30.
13. Krivokapitch J, Smith GT, Huang SC, et al. ^{13}N-ammonia myocardial imaging at rest and with exercise in normal volunteers. Circulation 1989;80: 1328–37.
14. Kuhle WG, Porenta G, Huang SC, et al. Quantification of regional myocardial blood flow using ^{13}N-ammonia and reoriented dynamic positron emission tomography. Circulation 1992;86:1004–17.
15. Tasca C, Stefaneanu L, Vasilescu C. The myocardial microangiopathy in human and experimental diabetes mellitus: a microscopic, ultra-structual, morphometric and computer-assisted symbolic-logic analysis. Endocrinologie 1986;24:59–69.
16. Downing SE, Lee JC, Weinstein EM. Coronary dilator actions of adenosine and CO_2 in experimental diabetes. Am J Physiol 1982;243:H252–8.
17. Lee JC, Downing SE. Coronary dynamics and myocardial metabolism in the diabetic newborn lamb. Am J Physiol 1979;237:H118–24.
18. Durante W, Sunahara FA, San AK. Effect of diabetes on metabolic coronary dilatation in the rat. Cardiovasc Res 1989;23:40–5.
19. Yamazaki Y, Kawamori R, Matsushima H, et al. Asymptomatic hyperglycemia is associated with increased intimal plus medial thickness of the carotid artery. Diabetologia 1995;38:585–91.
20. Kunjatjoor VV, Wilson DL, LeBoeuf RC. Increased atherosclerosis in streptozotocin-induced diabetic mice. J Clin Invest 1996;97:1767–73.
21. Samaha FF, Heinman FW, Ince C, Fleming J, Balaban RS. ATP-sensitive potassium channel is essential to maintain basal coronary tone in vivo. Am J Physiol 1992;262:C1220–7.
22. Aversano T, Ouyang P, Silverman H. Blockade of the ATP-sensitive hyperemia in the canine potassium channel modulates reactive hyperemia in the canine coronary circulation. Circ Res 1991;69:618–22.
23. Kanatsuka H, Sekiguchi N, Sato K, et al. Microvascular site for reactive hyperemia in the coronary circulation of the beating canine heart. Circ Res 1992;71:912–22.
24. Czernin J, Muller P, Chan S, et al. Influence of age and hemodynamics on myocardial blood flow and flow reserve. Circulation 1993;88:62–9.
25. Mintz GS, Painter JA, Pichard AD, et al. Atherosclerosis in angiographically normal coronary artery reference segments: an intravascular ultrasound study with clinical correlations. J Am Coll Cardiol 1995;25:1479–85.
26. Sakuma I, Akaishi Y, Fukao M, et al. Dipyridamole potentiates the anti-aggregating effect of endothelium-derived relaxing factor. Thromb Res Suppl 1990;12:87–90.
27. Bult H, Fret HRL, Jordeans FH, Herman AG. Dipyridamole potentiates the anti-aggregating and vasodilator activity of nitric oxide. Eur J Pharmacol 1991;199:1–8.
28. Kinsella JP, Torielli F, Ziegler JW, Ivy DD, Abman SH. Dipyridamole augmentation of response to nitric oxide. Lancet 1995;346:647–8.
29. Chan SY, Brunken RC, Czerrnin J, et al. Comparison of maximal myocardial blood flow during adenosine infusion with that of intravenous dipyridamole in normal men. J Am Coll Cardiol 1992;20:979–85.
30. Krivokapitch J, Stevenson L, Kobashigawa J, Huang S, Schelbert HR. Quantification of absolute myocardial perfusion at rest and during exercise with positron emission tomography after human cardiac transplantation. J Am Coll Cardiol 1991;18:512–7.
31. Chan SY, Kobashigawa J, Stevenson LW. Myocardial blood flow at rest and during pharmacological vasodilation in cardiac transplant during and after successful treatment of rejection. Circulation 1994;90:202–12.
32. Di Carli MF, Czernin J, Hoh CK, et al. Relation among stenosis severity, myocardial blood flow and flow reserve in patients with coronary artery disease. Circulation 1995;91:1944–51.
33. Czernin J, Auerbach M, Sun KT, Phelps M, Schelbert HR. Effects of modified pharmacologic stress approaches on hyperemic myocardial blood flow. J Nucl Med 1995;36:575–80.
34. Bottcher M, Czernin J, Sun KT, Phelps ME, Schelbert HR. Effect of caffeine on myocardial blood flow at rest and during pharmacological vasodilation. J Nucl Med 1995;36:2016–21.
35. Wu HM, Hoh CK, Buxton DB, et al. Quantification of myocardial blood flow using dynamic nitrogen-13-ammonia PET studies and factor analysis of dynamic structure. J Nucl Med 1995;36:2087–93.
36. Hutchins G, Schwaiger M, Rosenspire KC, Krivokapitch J, Schelbert HR, Kuhl DE. Noninvasive quantification of regional myocardial blood flow with N-13 ammonia and dynamic positron emission tomographic imaging. J Am Coll Cardiol 1990;15:1032–42.
37. Schelbert HR, Phelps ME, Huang SC, et al. N-13 ammonia as an indicator of myocardial blood flow. Circulation 1981;63:1259–72.
38. Krivokapitch J, Huang SC, Phelps ME, MacDonald NS, Shine KI. Dependence of $^{13}NH_3$ myocardial extraction and clearance on flow and metabolism. Am J Physiol 1982;242:H536–42.